DOI: 10.55415/deep-2023-0010.v1

Research article

Submission: AMM-2023-0003

Title: Smart-Responsive Carrier-Free Nanoassembly of SN38 Prodrug as Efficient Chemotherapeutic Nanomedicine

Author(s): *Guanting Li, Qianhui Jin, Fengli Xia, Shuwen Fu, Xuanbo Zhang, Hongying Xiao, Chutong Tian, Qingzhi Lv, Jin Sun, Zhonggui He* and Bingjun Sun**

Dear editor and reviewers,

We are truly grateful to your constructive comments and hard work. According to the comments and suggestions, we have made careful modifications on the original manuscript. The corrected portions in the revised manuscript have been highlighted in red. Below we summarized point-by-point responses to each of the comments/questions from the editor and the reviewers.

We appreciate the critical reviews of the manuscript and hope the revised version attached is improved to a significant degree to merit further consideration of publication.

Sincerely yours,
Bingjun Sun, Ph.D.
Professor, Department of Pharmaceutics
Wuya College of Innovation
Shenyang Pharmaceutical University, 110016, PR China
E-mail: sunbingjun_spy@sina.com

DOI: 10.55415/deep-2023-0010.v1

Reviewer: 1

Comments to the Author

The authors reported a smart-responsive SN38 prodrug nanoassembly for efficient cancer therapy. The SN38-SS-CST NPs potently defeated the growth of colon cancer without systemic toxicity, indicating a potential translational nanomedicine for chemotherapy. I think the results are interesting and can be published after minor modification.

1. As written, disulfide bond was reported to be a redox dual responsive chemical bond. Please explain what is the dual responsive.

Response: We appreciate the reviewer's comment. As an endogenous component of peptides and proteins, disulfide bond was first reported to possess reduction-responsiveness and was utilized to develop reduction-responsive prodrugs and nanomedicines.[1-2] Considering the similarity between disulfide bond and oxidation-responsive thioether bond, our group first proposed that disulfide bond could also facilitate oxidation-responsive drug release.[3] Therefore, disulfide bond is a chemical bond that could respond to both reductive and oxidative substances in the tumor microenvironments, thereby indicating a redox dual responsiveness.

Reference

[1] Maiti S, Park N, Han J H, et al. Gemcitabine–coumarin–biotin conjugates: a target specific theranostic anticancer prodrug[J]. Journal of the American Chemical Society, 2013, 135(11): 4567-4572.

[2] Zhang F, Zhu G, Jacobson O, et al. Transformative nanomedicine of an amphiphilic camptothecin prodrug for long circulation and high tumor uptake in cancer therapy[J]. Acs Nano, 2017, 11(9): 8838-8848.

[3] Sun B, Luo C, Yu H, et al. Disulfide bond-driven oxidation-and reduction-responsive prodrug nanoassemblies for cancer therapy[J]. Nano Letters, 2018, 18(6): 3643-3650.

DOI: 10.55415/deep-2023-0010.v1

2. Only a small amount of DSPE-PEG2k (20%, w/w) was added to reduce the free surface energy and improve stability. Does 20% represent the ratio of DSPE-PEG2k to the solution?

Response: We appreciate the reviewer's comment. The mass of DSPE-PEG_{2k} is equivalent to 20% of the total mass of SN38-SS-CST plus DSPE-PEG_{2k}, instead of 20% of the solution. In "4.3 Preparation and characterization of prodrug nanoassemblies", the exact mass to prepare nanoassemblies was described as: "Prodrug nanoassemblies of SN38-SS-CST were prepared by the typical one step nano-precipitation method. In brief, SN38-SS-CST (2 mg) was dissolved in 300 μL of acetone, and DSPE-PEG_{2k} (0.5 mg, 20% w/w) was dissolved in 100 μL of ethanol.".

3. For Nanoparticulate drug delivery systems, the recent literature might be updated, DOI:10.1016/j.jconrel.2020.09.035, DOI:10.1039/d1nh00506e.

Response: We appreciate the reviewer's comment. These literatures have been cited in the manuscript as ref [11] "" and ref [21] "".

4. The scale bar for figure 1c is not clear. Maybe a thicker scale bar can be added in the image.

Response: We agree with the reviewer's comment. The TME image of SN38-SS-CST NPs has been recaptured with a better view and the scale bar was also reprinted.

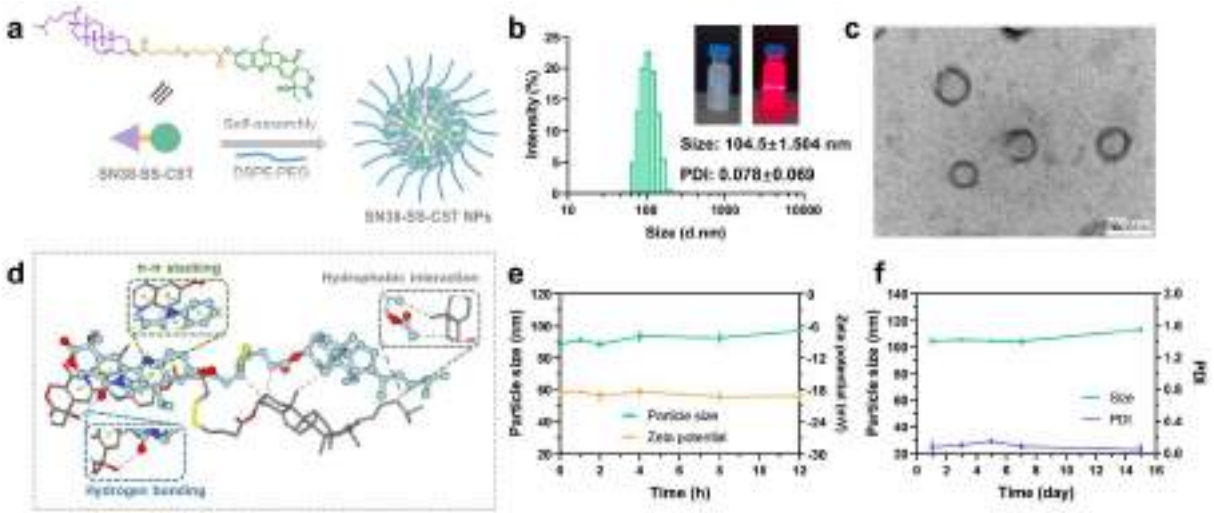

DOI: 10.55415/deep-2023-0010.v1

Figure 1. a) Schematic illustration of the self-assembly of SN38-SS-CST NPs. b) Size distribution and images of SN38-SS-CST NPs. c) TEM image of SN38-SS-CST NPs. Scale bar = 200 nm. d) Molecular dynamics simulations of the self-assembly of SN38-SS-CST NPs. Green lines indicate π-π stacking. Blue lines indicate hydrogen bonding. Grey lines indicate hydrophobic interactions. e) Colloidal stability of SN38-SS-CST NPs in PBS (pH 7.4) containing 10% FBS. f) Storage stability of SN38-SS-CST NPs at 4℃.

Reviewer: 2

Comments to the Author

Sun and co-workers reported a smart-responsive SN38 prodrug nano assemblies for efficient cancer therapy. In this work, SN38 was conjugated with an endogenous lipid cholesterol (CST) via a redox dual responsive disulfide bond. The prodrug could self-assemble into uniform prodrug nano assemblies with good colloidal stability and high drug loading. Moreover, by systematic experiments, SN38-SS-CST NPs potently defeated the growth of colon cancer without systemic toxicity, indicating a potential translational nanomedicine for chemotherapy. This manuscript can provide reference for further research. Contents are proper for publication after addressing the following problems.

Minor corrections:

1. Author claimed the self-assembled SN38-SS-CST NPs were spherical NPs round 100 nm. I think TEM image of figure 1c cannot provide sufficient evidence for this argument.

Response: We agree with the reviewer's comment. The TME image of SN38-SS-CST NPs has been recaptured with a better view.

DOI: 10.55415/deep-2023-0010.v1

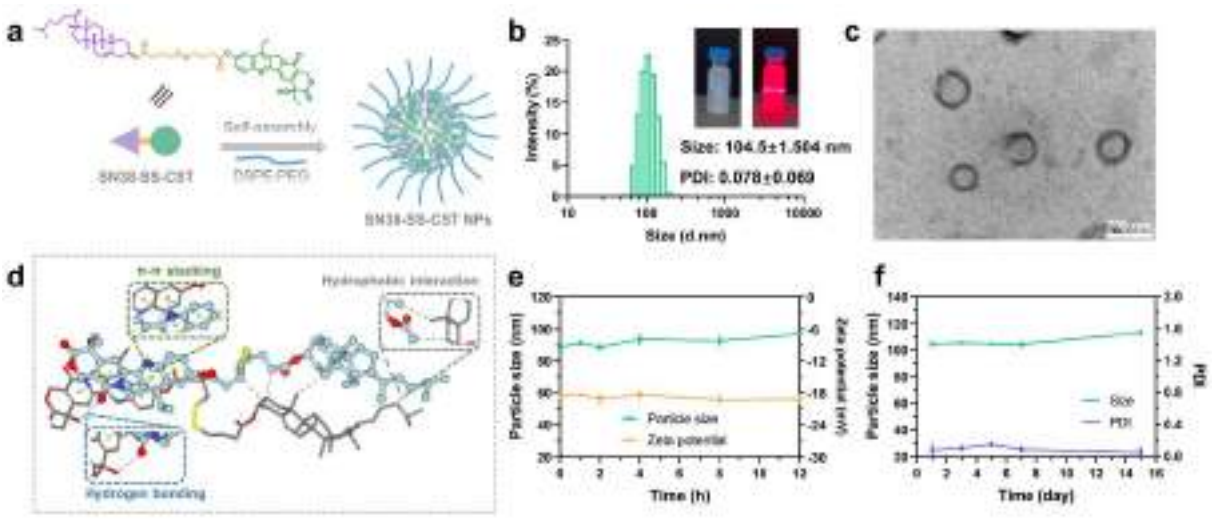

Figure 1. a) Schematic illustration of the self-assembly of SN38-SS-CST NPs. b) Size distribution and images of SN38-SS-CST NPs. c) TEM image of SN38-SS-CST NPs. Scale bar = 200 nm. d) Molecular dynamics simulations of the self-assembly of SN38-SS-CST NPs. Green lines indicate π-π stacking. Blue lines indicate hydrogen bonding. Grey lines indicate hydrophobic interactions. e) Colloidal stability of SN38-SS-CST NPs in PBS (pH 7.4) containing 10% FBS. f) Storage stability of SN38-SS-CST NPs at 4℃.

2. Basis sets and algorithms of molecular dynamics simulation should be provided in main article.

Response: We appreciate the reviewer's comment. The detailed parameters of the simulation were supplemented in "4.4 Self-assembly mechanisms" as: "The self-assembly mechanisms of SN38-SS-CST NPs were investigated using molecular dynamics simulations. First, the 3-dimentional conformation of SN38-SS-CST was assesses using Sybyl software. Then, the self-assembly process of SN38-SS-CST NPs was analyzed using Discovery Studio 2017 Visualizer software. The simulated box center parameter was (-6.049, 0.406, 0.869). The simulated box size parameter was (48.897, 40.062, 39.957). The maximum output conformation number is 9.".

3. Author claimed, SN38-SS-CST NPs remained stable with almost no changes in particle size during the 12 h incubation. I think the change of zeta potential was also important data for verify the stability of nano-agents.

DOI: 10.55415/deep-2023-0010.v1

Response: We agree the reviewer's comment. The zeta potential changes of SN38-SS-CST NPs have been supplemented in Figure 1e. The manuscript has been modified in "2.4 Colloidal stability" as: "In addition, to stimulate the in vivo condition, PBS (pH 7.4) containing 10% FBS was unitized as media to incubate with SN38-SS-CST NPs. As shown in Figure 1e, SN38-SS-CST NPs remained stable with almost no changes in particle size and zeta potential during the 12 h incubation. The results indicated that SN38-SS-CST NPs had superior in vitro and in vivo colloidal stability.".

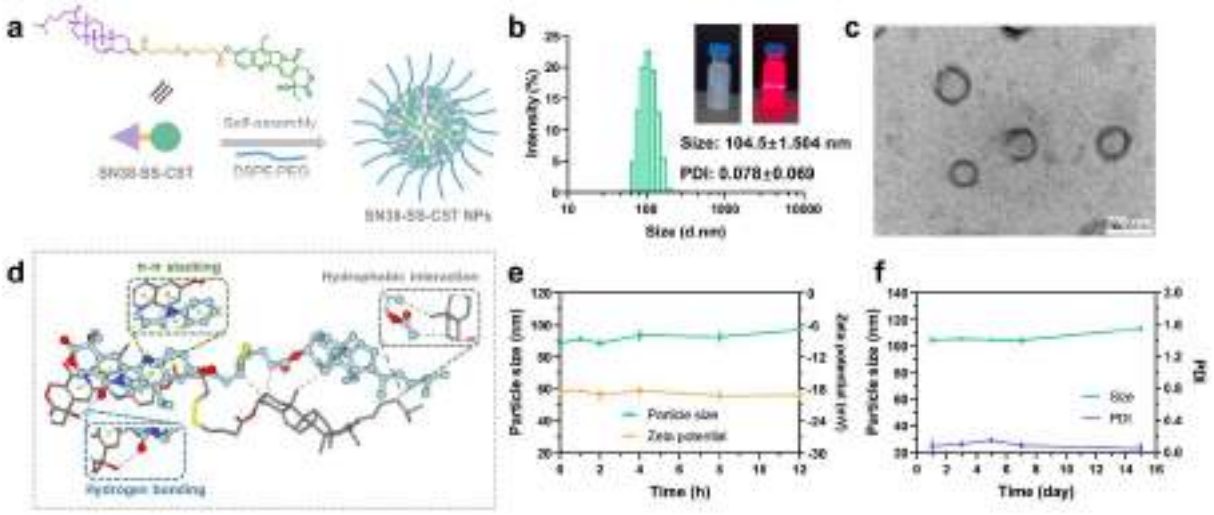

Figure 1. a) Schematic illustration of the self-assembly of SN38-SS-CST NPs. b) Size distribution and images of SN38-SS-CST NPs. c) TEM image of SN38-SS-CST NPs. Scale bar = 200 nm. d) Molecular dynamics simulations of the self-assembly of SN38-SS-CST NPs. Green lines indicate π-π stacking. Blue lines indicate hydrogen bonding. Grey lines indicate hydrophobic interactions. e) Colloidal stability of SN38-SS-CST NPs in PBS (pH 7.4) containing 10% FBS. f) Storage stability of SN38-SS-CST NPs at 4℃.

4. Mice survival time curves should be provided.

Response: We appreciate the reviewer's comment. The in vivo antitumor experiment lasted for 11 days from first injection to mice sacrifice. During this period, no premature death was found in all groups. More importantly, according to the ethical concern, the experiment has to stop at the 11th day because the tumor volume of the mice in PBS group has reached 2000 mm^3. Therefore, the mice in all groups had a 100% survival rate throughout the experiment.

DOI: 10.55415/deep-2023-0010.v1

5. Author can improve the signal intensity of ^{1}H NMR spectra for SN38-SS-CST.

Response: We appreciate the reviewer's comment. The ^{1}H NMR spectra for SN38-SS-CST has been replaced with improved signal intensity.

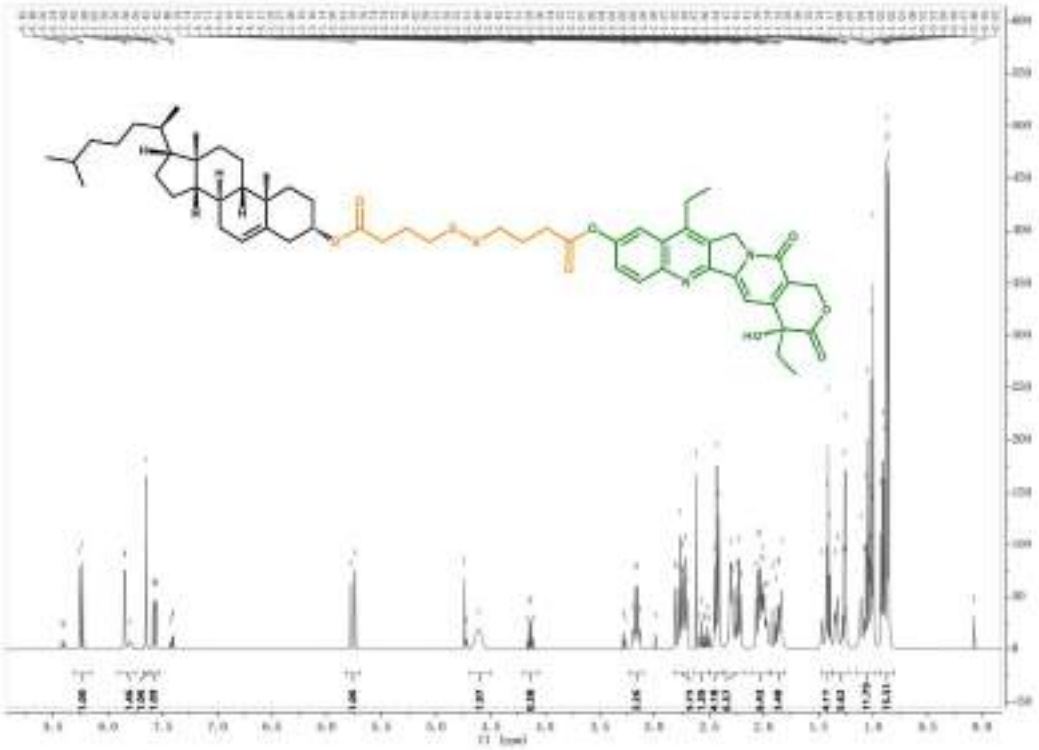

Figure S4. ^{1}H NMR of SN38-SS-CST. ^{1}H NMR (400 MHz, Chloroform-*d*) δ 8.25 (d, *J* = 9.2 Hz, 1H, Ar-H), 7.85 (d, *J* = 2.5 Hz, 1H, Ar-H), 7.65 (s, 1H, Ar-H), 7.57 (dd, *J* = 9.1, 2.5 Hz, 1H, Ar-H), 5.76 (d, *J* = 16.3 Hz, 1H, -CH), 4.59 (s, 3H), 4.17-4.11 (m, 1H, -CH), 3.17 (q, *J* = 8.3 Hz, 2H), 2.85 - 2.74 (m, 6H, -CH_2), 2.64 - 2.48 (m, 3H), 2.42 (q, *J* = 7.6 Hz, 4H), 2.27 (d, *J* = 32.4 Hz, 6H), 2.05 (s, 6H), 1.92 (s, 3H), 1.41 (s, 4H), 1.25 (s, 6H), 1.03 (dd, *J* = 19.5, 8.7 Hz, 12H), 0.95 - 0.83 (m, 15H, -CH_3).

6. HRMS of SN38-SS-CST can be displayed from 0-1000(m/z) to show the compound purity.

Response: We appreciate the reviewer's comment. The HRMS spectra from 0-2000 (m/z) was shown below. However, the response of MS is influenced by many factors, as well as the production of large numbers of fragment ions. Therefore, the MS spectra is not indicative of

DOI: 10.55415/deep-2023-0010.v1

the purity of the compound. To characterize the purity of the prodrug, high performance liquid chromatography (HPLC) was utilized. The HPLC spectra was shown in Figure S6. The manuscript was modified in "2.1 Chemical synthesis" as: "According to ^{1}H nuclear magnetic resonance spectroscopy (NMR) and mass spectrometry (MS), intermediate CST-SS-COOH and SN38-SS-CST were successfully synthesized (Figure S2-5). The purity of SN38-SS-CST could reach 99.74% (Figure S6).".

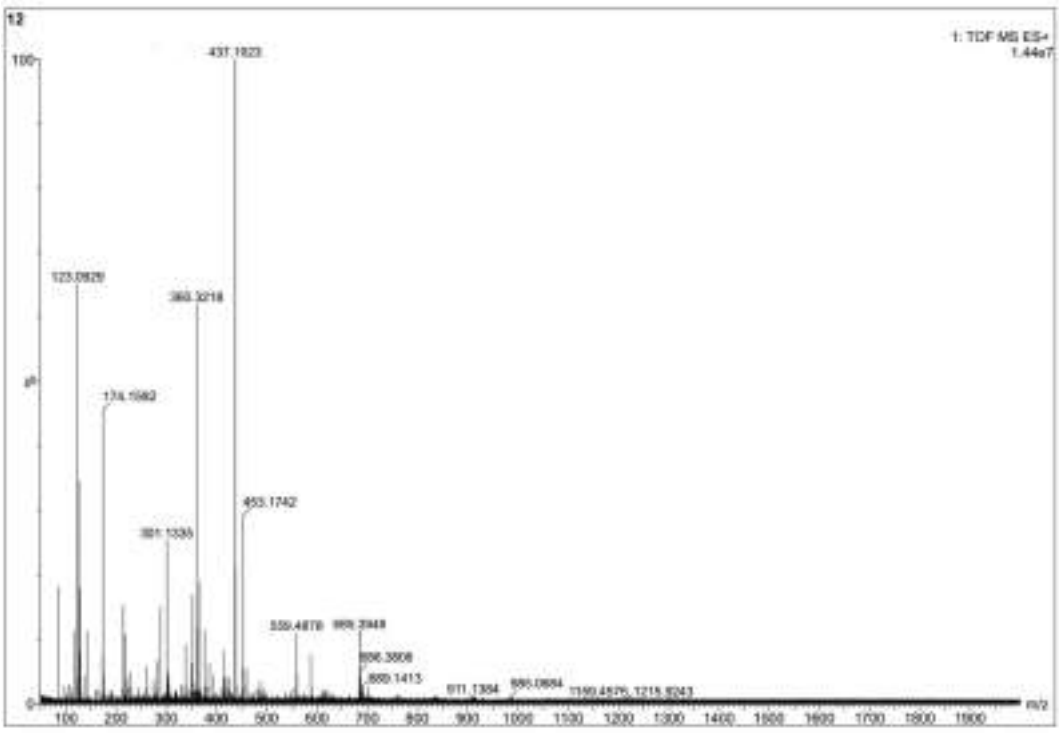

Figure. HRMS spectra from 0-2000 (m/z) of SN38-SS-CST.

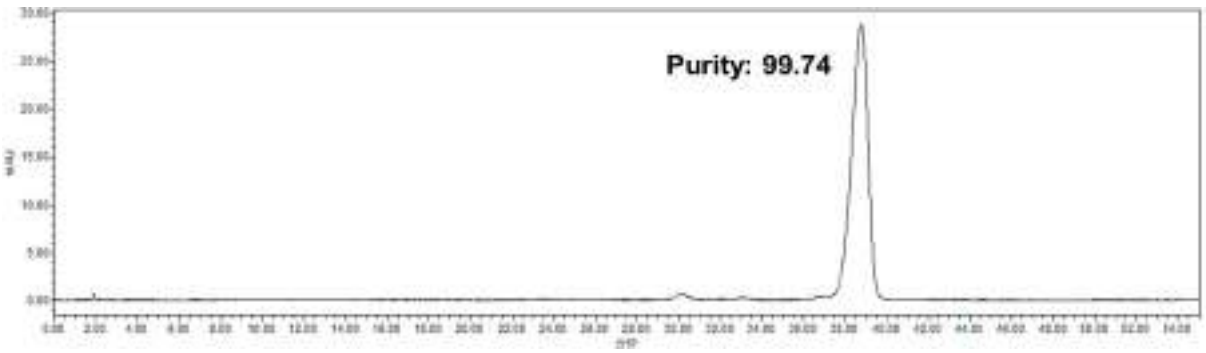

Figure S6. HPLC spectra of SN38-SS-CST. Purity: 99.74%.

DOI: 10.55415/deep-2023-0010.v1

7. Blood biochemical indicators of mice were only showed by ALT, AST, CREA and UREA. It was recommended to add more indicators for clarification as well as additional blood tests (e.g., white blood cells, red blood cells, platelets, etc.) to confirm biocompatibility.

Response: We appreciate the reviewer's comment. The blood tests are important indicators to evaluate the biocompatibility of the formulations. However, our institution was seriously forbidden because of the corona virus when we conducted the animal experiments. Under this circumstance, the blood samples could not be sent to the facility for testing. Therefore, the blood tests were not covered in this manuscript.

Reviewer: 3

Comments to the Author

In this work, a novel cholesterol-conjugated SN38 prodrug was reported. SN38-SS-CST could self-assemble into prodrug nanoassemblies with a high drug loading of 32%. The authors carried out a series of work to investigate the antitumor effectiveness of the SN38-SS-CST NPs and the figures were nicely made. This work provided new insight into developing translational nanomedicine. Before publication in Acta Materia Medica, some issues have to be addressed.

1. This work only contained a disulfide-bridged prodrug. A lot of novel chemical bonds have been reported to have redox-responsive characteristics, such as trisulfide and diselenide. Why was only disulfide covered in this work?

Response: We appreciate the reviewer's comment. In this work, we intended to develop a translational SN38 prodrug nanomedicine. In our previous work, diselenide bond and trisulfide bond have been constructed into prodrug nanoassemblies with multiple therapeutic advantages.[1-2] However, to our knowledge, both diselenide bond- and trisulfide bond-based chemical linkages have to be prepared by chemical synthesis. In contrast, disulfide bond-based chemical linkages are commercial products, which is more conductive to industrial production, quality control and cost control. Therefore, in this work, we focused on

DOI: 10.55415/deep-2023-0010.v1

disulfide-bridged SN38 prodrug nanoassemblies and evaluated their potential as translational nanomedicine.

References

[1] Sun B, Luo C, Zhang X, et al. Probing the impact of sulfur/selenium/carbon linkages on prodrug nanoassemblies for cancer therapy[J]. Nature Communications, 2019, 10(1): 3211.

[2] Yang Y, Sun B, Zuo S, et al. Trisulfide bond–mediated doxorubicin dimeric prodrug nanoassemblies with high drug loading, high self-assembly stability, and high tumor selectivity[J]. Science advances, 2020, 6(45): eabc1725.

2. The MS spectrum of CST-SS-COOH should also be provided.

Response: We agree with the reviewer's comment. The MS spectrum of CST-SS-COOH was provided in Figure S3.

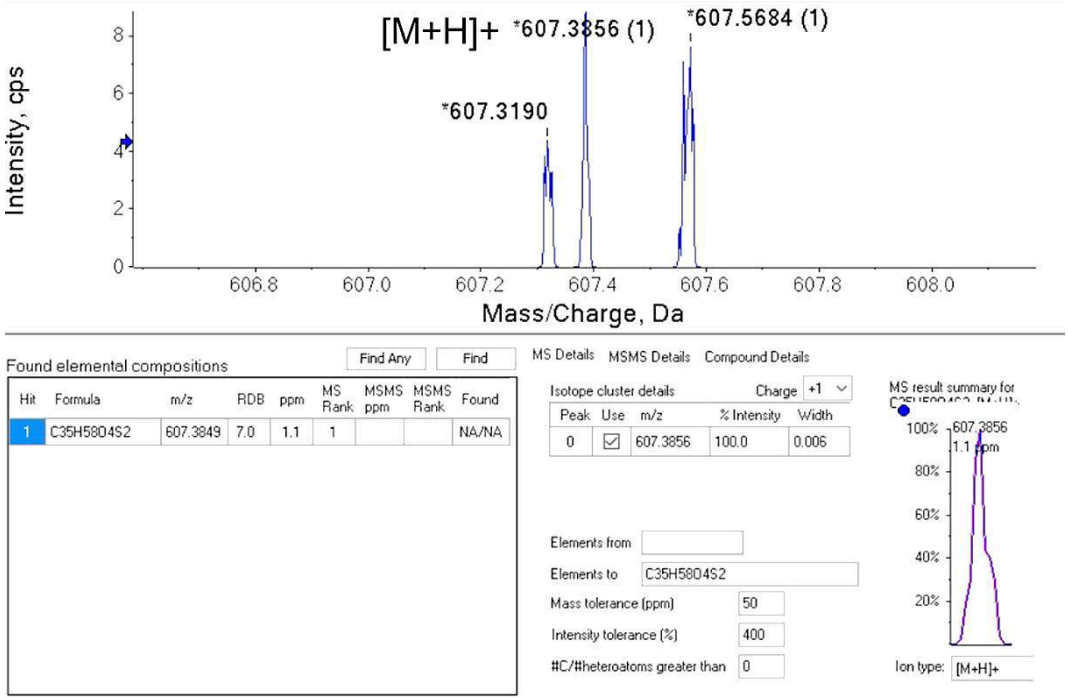

Figure S3. MS of CST-SS-COOH. Calcd for $C_{35}H_{58}O_4S_2$, 607.3849; found, 607.3856 $[M+H]^+$.

DOI: 10.55415/deep-2023-0010.v1

3. The TEM images of SN38-SS-CST NPs are not clear. A new image should be provided.

Response: We agree with the reviewer's comment. The TME image of SN38-SS-CST NPs has been recaptured with a better view.

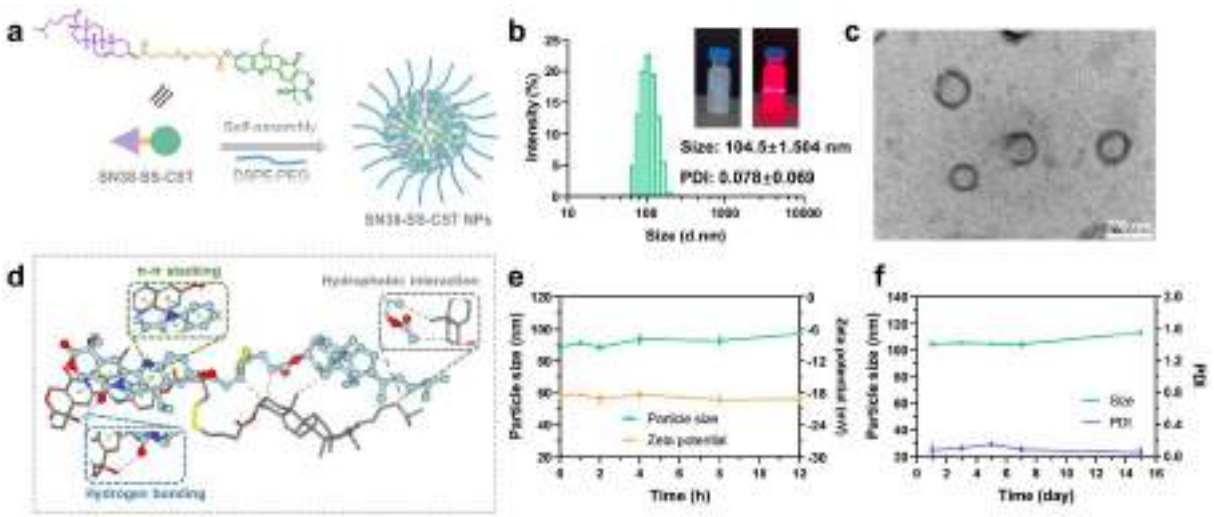

Figure 1. a) Schematic illustration of the self-assembly of SN38-SS-CST NPs. b) Size distribution and images of SN38-SS-CST NPs. c) TEM image of SN38-SS-CST NPs. Scale bar = 200 nm. d) Molecular dynamics simulations of the self-assembly of SN38-SS-CST NPs. Green lines indicate π-π stacking. Blue lines indicate hydrogen bonding. Grey lines indicate hydrophobic interactions. e) Colloidal stability of SN38-SS-CST NPs in PBS (pH 7.4) containing 10% FBS. f) Storage stability of SN38-SS-CST NPs at 4℃.

4. As introduced in the introduction part, irinotecan was approved by FDA for the treatment of colorectal cancer. Why were 4T1 cells selected for cytotoxicity study?

Response: We appreciated the reviewer's comment. Although irinotecan or SN38 and their related formulations have not been yet approved for the treatment of breast cancers, we intended to investigate the antitumor performance of our formulation on other tumor cell lines. As shown in Table S3, SN38-SS-CST NPs were more cytotoxic on both CT26 colorectal tumor cells and 4T1 breast tumor cells, indicating a potent and broad-spectrum antitumor platform.

DOI: 10.55415/deep-2023-0010.v1

Table S3. IC_{50} values of the formulations.

Formulations	IC_{50} on CT26 cell (nM)	IC_{50} on 4T1 cell (nM)
Campto	2063	2638
SN38-SS-CST NPs	291.2	335.7

5. The release mechanisms should be described in detail in the figure legend or in the main text.

Response: We agree with the reviewer's comment. The detailed release mechanisms were put forward in the legend of Figure 2a as: "Figure 2. a) Proposed release mechanisms of SN38-SS-CST NPs. In GSH media, SN38-sulfhydryl compound (SN38-SH) was first released through the sulfur exchange between SN38-SS-CST and GSH. The exposed sulfhydryl of SN38-SH would attack the adjacent ester bond for intramolecular cyclization, which then released SN38. In ROS media, the disulfide would be oxidized into hydrophilic sulfoxide or sulphone, thereby facilitating the hydrolysis of the adjacent ester bond to release SN38.".

DOI: 10.55415/deep-2023-0010.v1

Title

Smart-Responsive Carrier-Free Nanoassembly of SN38 Prodrug as Efficient Chemotherapeutic Nanomedicine

Guanting Li[a], Qianhui Jin[a], Fengli Xia[a], Shuwen Fu[b], Xuanbo Zhang[a], Hongying Xiao[a], Chutong Tian[a], Qingzhi Lv[c], Jin Sun[a], Zhonggui He[a,] and Bingjun Sun[a,*]*

Affiliation

a. Department of Pharmaceutics, Wuya College of Innovation, Shenyang Pharmaceutical University, Shenyang 110016, P. R. China

b. School of Pharmacy, Shenyang Pharmaceutical University, Shenyang 110016, P. R. China

c. School of Pharmacy, Binzhou Medical University, Yantai 264000, P. R. China

[*]Correspondence: hezhgui_student@aliyun.com (Z. He); sunbingjun_spy@sina.com (B. Sun)

DOI: 10.55415/deep-2023-0010.v1

Graphical abstract

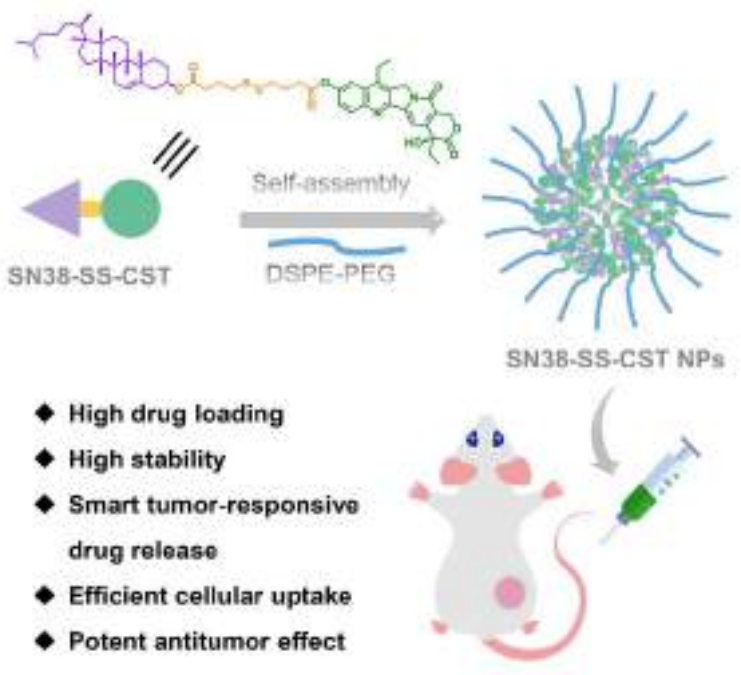

Highlights

- A novel SN38 prodrug that could self-assemble into prodrug nanoassemblies independent of carrier materials is reported.
- SN38 prodrug nanoassemblies could specifically release active SN38 in response to the overexpressed redox inside tumor tissues, while remain intact in other normal tissues.
- The smart-responsive SN38 prodrug nanoassemblies significantly improve antitumor outcomes than commercial Campto®.

In brief

A smart-responsive SN38 prodrug nanoassembly for efficient cancer therapy was reported. SN38 prodrug nanoassemblies indicate multiple therapeutic advances including ultrahigh drug loading, good colloidal stability, tumor-specific drug release, increased cellular uptake, thereby potently defeating the growth of colon cancer without systemic toxicity.

DOI: 10.55415/deep-2023-0010.v1

ABSTRACT

7-ethyl-10-hydroxy-camptothecin (SN38) is a broad-spectrum antitumor agent. Unfortunately, the application of SN38 is greatly limited by its poor solubility. In response, irinotecan, the hydrophilic derived prodrug of SN38, has been developed into commercial formulation Campto® for the treatment of colorectal cancer. However, only 1% to 0.1% of irinotecan could be transferred to active SN38 in vivo, leading to the unsatisfactory antitumor activity in clinic. Herein, we report a smart-responsive SN38 prodrug nanoassembly for efficient cancer therapy. First, SN38 was conjugated with an endogenous lipid cholesterol (CST) via a redox dual-responsive disulfide bond (SN38-SS-CST). The prodrug could self-assemble into uniform prodrug nanoassemblies with good colloidal stability and ultrahigh drug loading. Under the redox environments of tumor cells, SN38-SS-CST NPs could sufficiently release SN38 while keep intact in normal tissues. Finally, SN38-SS-CST NPs potently defeated the growth of colon cancer without systemic toxicity, promising a translational chemotherapeutic nanomedicine.

Keywords: Prodrug nanoassembly, SN38, Redox responsiveness, Nanomedicine, Cancer therapy

DOI: 10.55415/deep-2023-0010.v1

1. INTRODUCTION

Chemotherapy has always been the first-line choice for cancer treatment [1]. Among the various cytotoxic chemo-drugs, 7-ethyl-10-hydroxy-camptothecin (SN38), a semi-synthetic camptothecin derivative, has a broad and potent antitumor efficacy by inhibiting the activity of topoisomerase I to cause lethal DNA damage [2]. However, as the extremely hydrophobic characteristic, the application of SN38 was severely limited by the poor solubility. Although the carboxylic acid ester form of SN38 could improve the solubility, the system toxicity will also be increased [3, 4]. Under the circumstances, the water-soluble derivative of SN38, irinotecan (Campto®) was developed and approved by FDA for the treatment of colorectal cancer [5]. Irinotecan was synthesized by conjugating SN38 with a 4-piperidinopiperidine group via an easter bond. To exert cytotoxicity, irinotecan has to be converted to active SN38 through the cleavage of the easter bond. Unfortunately, the hydrolysis of easter bond was so inefficient in vivo that only 1% to 0.1% of irinotecan could be metabolized into SN38, thereby greatly impeding the antitumor activity of irinotecan [6]. Resultingly, the cytotoxicity of irinotecan was 100 to 1000-fold lower than that of SN38 [7].

Nanoparticulate drug delivery systems (Nano-DDSs) have been one of the most successful attempts to facilitate chemotherapy [8-11]. The well-designed Nano-DDSs could protect the loaded drug from premature metabolism and clearance, and improve tumor accumulation through the known enhanced permeability and retention (EPR) effect [12, 13]. Conventional Nano-DDSs (e.g., liposomes and microspheres) usually encapsulate the drugs through the intermolecular nonvalent interactions such as hydrophobic interactions and electrostatic interactions between carrier materials and drugs [14, 15]. However, SN38 has an extremely flat and highly rigid structure with high crystallization trend [16]. Therefore, SN38 showed a very low affinity with the carrier materials, resulting in the low drug loading efficiency, poor stability and premature drug leakage. In addition, the overused carrier materials may introduce carrier-related allergy and toxicity [17]. Rational design of SN38-based nanomedicines remains a challenge.

Recently, prodrug nanoassemblies have emerged to serve as a versatile nanoplatform for antitumor drug delivery [18]. Through the simple one-step nanoprecipitation method, prodrug molecules could self-assemble into nano-sized assemblies independent of carrier materials

DOI: 10.55415/deep-2023-0010.v1

[19]. Prodrug nanoassemblies act as both the carrier and the cargo with ultra-high drug loading (> 30%) and negligible carrier-related adverse effects [18]. Additionally, the facile fabrication helps to remove the barrier for industrial translation. More importantly, according to the characteristics of the tumor microenvironment (TME), smart tumor stimuli-responsive prodrugs have been wildly developed to facilitate tumor-specific drug release [20, 21]. Integrating both the merits of the two techniques, stimuli-responsive prodrug nanoassemblies represent a potent and safe antitumor platform.

Herein, we report a smart-responsive SN38 prodrug nanoassemblies for efficient cancer therapy. SN38 was conjugated with an endogenous lipid cholesterol (CST) via a redox dual-responsive disulfide bond (termed as SN38-SS-CST). Using the one-step nanoprecipitation method, SN38-SS-CST could self-assemble into nanoassemblies (SN38-SS-CST NPs) around 100 nm driven by hydrophobic interactions, π-π stacking and hydrogen bonding. Under the redox-overexpressed TME, SN38-SS-CST NPs could sufficiently release SN38 and showed no burst release under normal physiological conditions. Finally, SN38-SS-CST NPs potently defeated the growth of colon cancer without systemic toxicity, indicating a potential translational nanomedicine for chemotherapy.

2. RESULTS AND DISCUSSIONS

2.1 Chemical synthesis

To construct self-assembling prodrug, CST was chosen as the modifying side chain to conjugating with SN38 (Figure S1). In addition, disulfide bond was reported to be a redox dual-responsive chemical bond, which could facilitate tumor specific drug release profiles [22]. On the basis, we developed disulfide-bridged SN38-SS-CST prodrug. According to ^{1}H nuclear magnetic resonance spectroscopy (NMR) and mass spectrometry (MS), intermediate CST-SS-COOH and SN38-SS-CST were successfully synthesized (Figure S2-5). The purity of SN38-SS-CST could reach 99.74% (Figure S6).

2.2 Characterization of prodrug nanoassemblies

As shown in Figure 1a, SN38-SS-CST self-assembled into prodrug nanoassemblies using the one step nanoprecipitation method independent of carrier materials. Only a small amount of

DOI: 10.55415/deep-2023-0010.v1

DSPE-PEG$_{2k}$ (20%, w/w) was added to reduce the free surface energy and improve stability. The self-assembled SN38-SS-CST NPs were spherical NPs round 100 nm (Figure 1b-c and Table S1) with an ultrahigh drug loading of 31.94%. After laser irradiation, SN38-SS-CST NPs showed obvious Tyndall effect, indicating the colloidal property. In addition, the negative zeta protentional (-22.3 mV) could help to maintain the colloidal stability of prodrug nanoassemblies.

2.3 Self-assembly mechanisms

The self-assembly process of SN38-SS-CST NPs was analyzed using molecular dynamics simulations. According to the conformation of the prodrug molecules (Figure 1d), it could be revealed that during the self-assembly process, the aromatic rings of S38 molecules were packed through π-π stacking interactions and the CST molecules were clustered together under hydrophobic interactions. In addition, the hydroxyl groups of SN38 provided the hydrogen bonding. The molecular dynamics simulation diameters also verified the spontaneous self-assembly of SN38-SS-CST (a negative grid score and a positive internal energy repulsive) and the process was mainly driven by Van der Waals forces (Table S2).

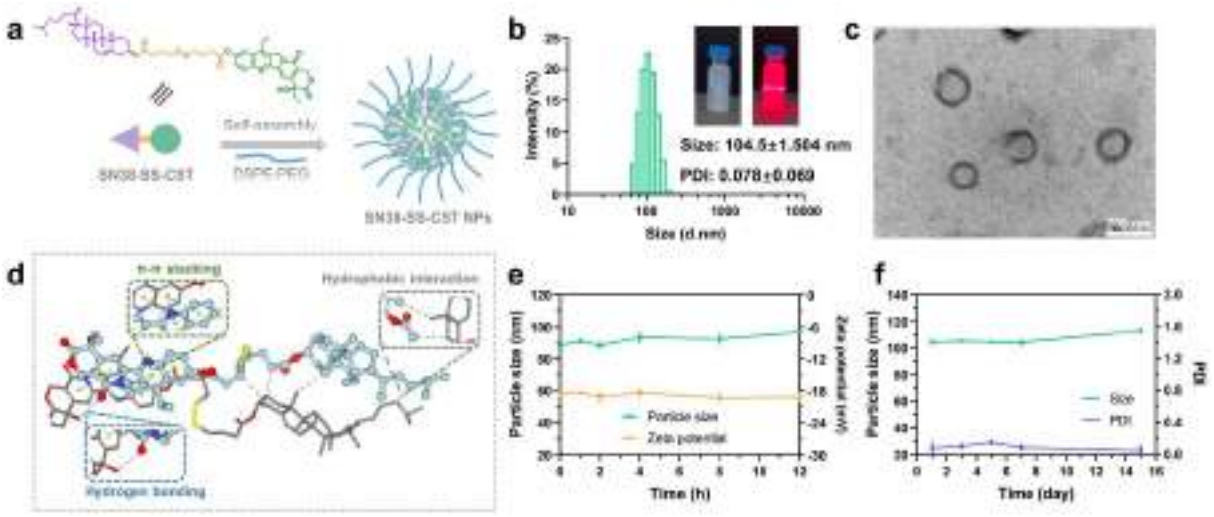

Figure 1. a) Schematic illustration of the self-assembly of SN38-SS-CST NPs. b) Size distribution and images of SN38-SS-CST NPs. c) TEM image of SN38-SS-CST NPs. Scale bar = 200 nm. d) Molecular dynamics simulations of the self-assembly of SN38-SS-CST NPs. Green lines indicate π-π stacking. Blue lines indicate hydrogen bonding. Grey lines indicate

DOI: 10.55415/deep-2023-0010.v1

hydrophobic interactions. e) Colloidal stability of SN38-SS-CST NPs in PBS (pH 7.4) containing 10% FBS. f) Storage stability of SN38-SS-CST NPs at 4℃.

2.4 Colloidal stability

First, we investigated the storage stability of SN38-SS-CST NPs at 4℃. During the half-month storage, no obvious changes in particle size were observed indicating that SN38-SS-CST NPs could be long-time stored for future use (Figure 1f). In addition, to stimulate the in vivo condition, PBS (pH 7.4) containing 10% FBS was unitized as media to incubate with SN38-SS-CST NPs. As shown in Figure 1e, SN38-SS-CST NPs remained stable with almost no changes in particle size and zeta potential during the 12 h incubation. The results indicated that SN38-SS-CST NPs had superior in vitro and in vivo colloidal stability.

2.5 In vitro drug release

Ideally, we hope prodrugs could release active parent drugs in targeted sites but remain intact in other cells and tissues [23]. It was well known that both oxidative reactive oxygen species (ROS) and reductive glutathione (GSH) are overexpressed in the TME [24]. In response, various tumor-specific stimuli responsive chemical bonds were developed for smart antitumor prodrugs and nanomedicines [25, 26]. Among them, disulfide bond has been reported to have redox dual-responsiveness [27, 28]. Therefore, we introduced disulfide bond in the SN38-SS-CST prodrug. According to the previous research [27], the release mechanisms were illustrated in Figure 2a.

The stimuli-responsive drug release profiles of SN38-SS-CST NPs was investigated using H_2O_2 as ROS stimuli and DTT as GSH stimuli. As depicted in Figure 2b-c, the stimuli release of SN38 was in a time-dependent and concentration-dependent behavior. Compared with ROS as stimuli, SN38-SS-CST NPs indicated much better reduction-responsiveness. About 60% of SN38 was released in the presentence of 10 mM DTT in 24 h. Notably, there was almost no burst release of SN38 without the absence of stimuli, demonstrating a superior selectivity of SN38-SS-CST NPs towards redox-overexpressed tumor cells and normal cells.

DOI: 10.55415/deep-2023-0010.v1

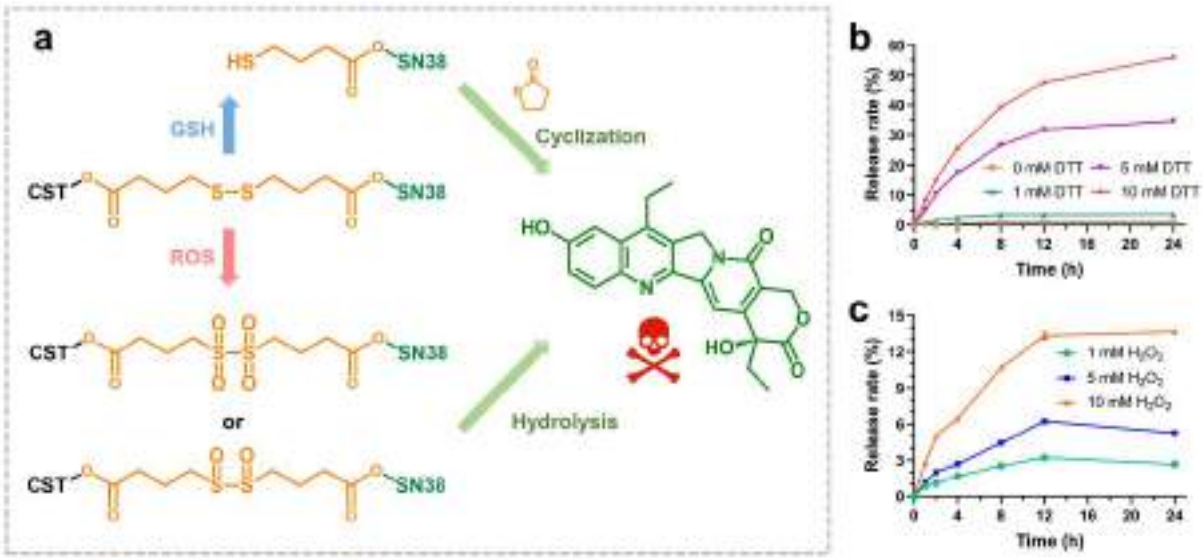

Figure 2. a) Proposed release mechanisms of SN38-SS-CST NPs. In GSH media, SN38-sulfhydryl compound (SN38-SH) was first released through the sulfur exchange between SN38-SS-CST and GSH. The exposed sulfhydryl of SN38-SH would attack the adjacent ester bond for intramolecular cyclization, which then released SN38. In ROS media, the disulfide would be oxidized into hydrophilic sulfoxide or sulphone, thereby facilitating the hydrolysis of the adjacent ester bond to release SN38. b) GSH stimuli-responsive release profiles of SN38-SS-CST NPs. c) ROS stimuli-responsive release profiles of SN38-SS-CST NPs. Data are presented as means ± SD (n = 3).

2.6 Cytotoxicity

The cytotoxicity of SN38-SS-CST NPs and Campto was compared on CT26 and 4T1 cells. As shown in Figure 3a-b and Table S3, the half maximal inhibitory concentration (IC_{50}) of Campto (2063 nM on CT26 cells; 2638 nM on 4T1 cells) was much higher than that of SN38-SS-CST NPs (291.2 nM on CT26 cells; 335.7 nM on 4T1 cells). The poor cytotoxicity of Campto could be attributed to the slow hydrolysis rate of the easter bond of irinotecan, leading to the slow and inefficient release of active SN38. In contrast, SN38-SS-CST NPs could rapidly and sufficiently release SN38 in tumor cells, thereby yielding a potent cytotoxicity.

2.7 Cellular uptake

DOI: 10.55415/deep-2023-0010.v1

The cellular uptake efficiency of prodrug nanoassemblies was investigated on CT26 cells. Free coumarin-6 (C-6) solution and C-6-labeled SN38-SS-CST NPs were given to CT26 cells and incubated for 0.5 h or 2 h. Then, the intracellular fluorescence intensity was evaluated by confocal laser scanning microscopy (CLSM). As displayed in Figure 3c, it was obviously observed that the intracellular fluorescence intensity of C-6-labeled SN38-SS-CST NPs was much higher than that of free C-6 solution at both time intervals. This result indicated that prodrug nanoassemblies could be more sufficiently endocytosed by tumor cells.

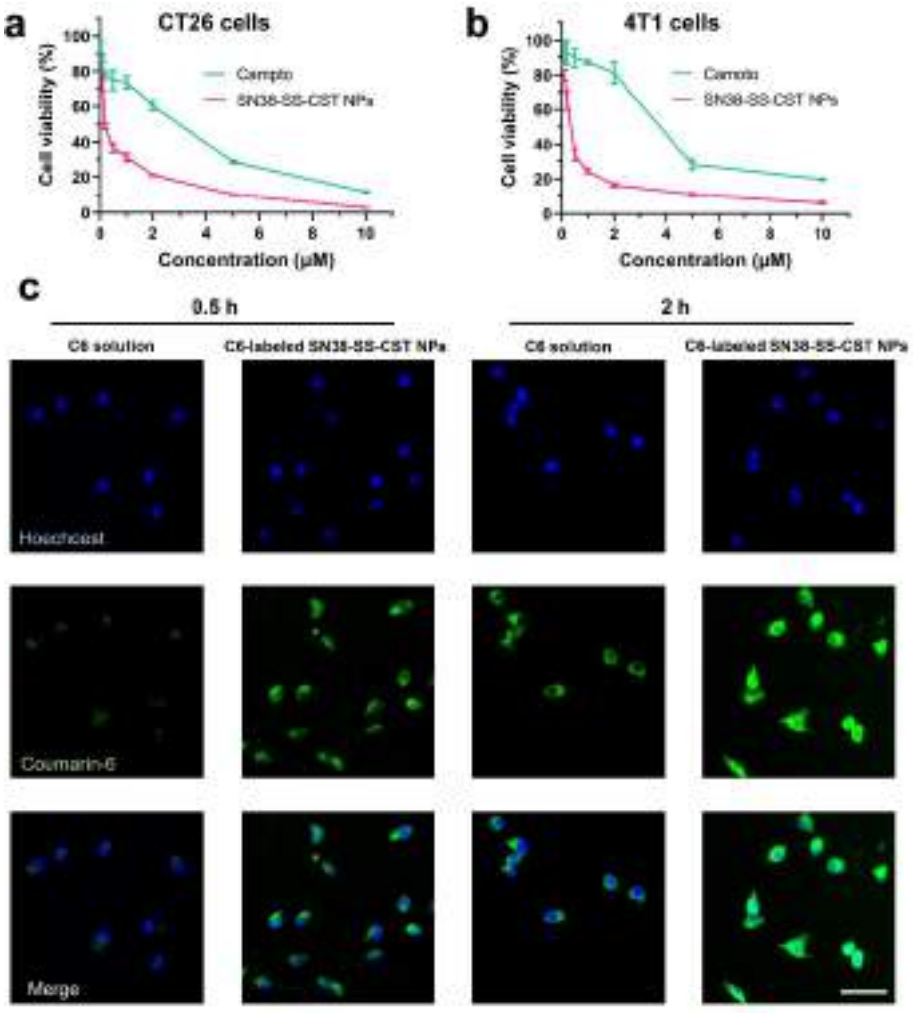

Figure 3. a) Cell viability of the formulations on CT26 cells. b) Cell viability of the formulations on 4T1 cells. Data are presented as means ± SD (n = 3). c) CLSM images of CT26 cells incubated with free C-6 or C-6-labeled SN38-SS-CST NPs for 0.5 h and 2 h. Scale bar = 50 μm.

DOI: 10.55415/deep-2023-0010.v1

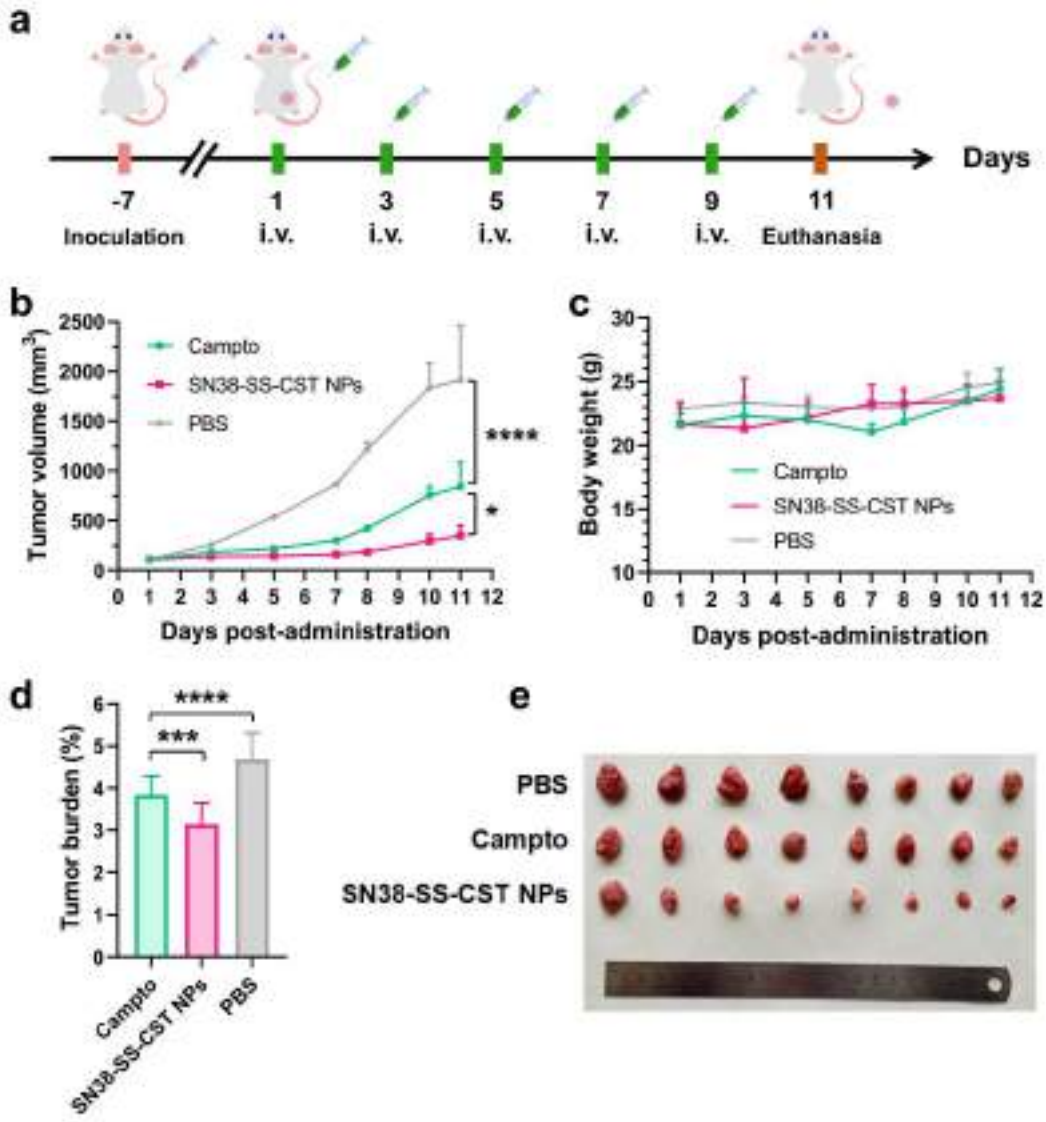

Figure 4. a) Pharmacodynamics study protocol. b) Tumor volume of CT26 bearing mice during the treatment. c) Body weigh changes of CT26 bearing mice during the treatment. d) Tumor burden of CT26 bearing mice at the end of the treatment. e) Images of resected CT26 tumors at the end of treatment. Data are presented as means ± SD (n = 8), *$p < 0.05$, ***$p < 0.001$, ****$p < 0.0001$.

2.8 In vivo antitumor effect

The in vivo antitumor efficacy of SN38-SS-CST NPs was investigated on xenograft CT26 bearing BALB/c mice. The formulations were given to the mice every other day for total five injections (Figure 4a). As shown in Figure 4b and d-e, CT26 tumors rapidly and unrestrictedly grew in the PBS-treating group. Commercial Campto moderately inhibited tumor growth, but

DOI: 10.55415/deep-2023-0010.v1

the tumor volume still reached around 800 mm^3 at the end of treatment. In comparation, SN38-SS-CST NPs indicated potent tumor inhibitory effect in terms of both tumor volume and tumor burden. The H&E staining of tumors revealed that SN38-SS-CST NPs-treated group had more necrotic areas (Figure 5). In addition, the immunofluorescence illustrated that SN38-SS-CST NPs successfully inhibited tumor proliferation (ki67) and induced more tumor apoptosis (Tunel).

The systemic toxicity was evaluated by body weight, hepatorenal functions and H&E staining of main organs. Both formulations did not lead to body weight changes, hepatorenal damage and discernible histological lesions in main organs (Figure 4c and Figure S7-8), indicating the superior safety of SN38-SS-CST NPs. Overall, SN38-SS-CST NPs overcame the dilemma of commercial formulation Campto and presented a safe and potent antitumor platform with translational prospective.

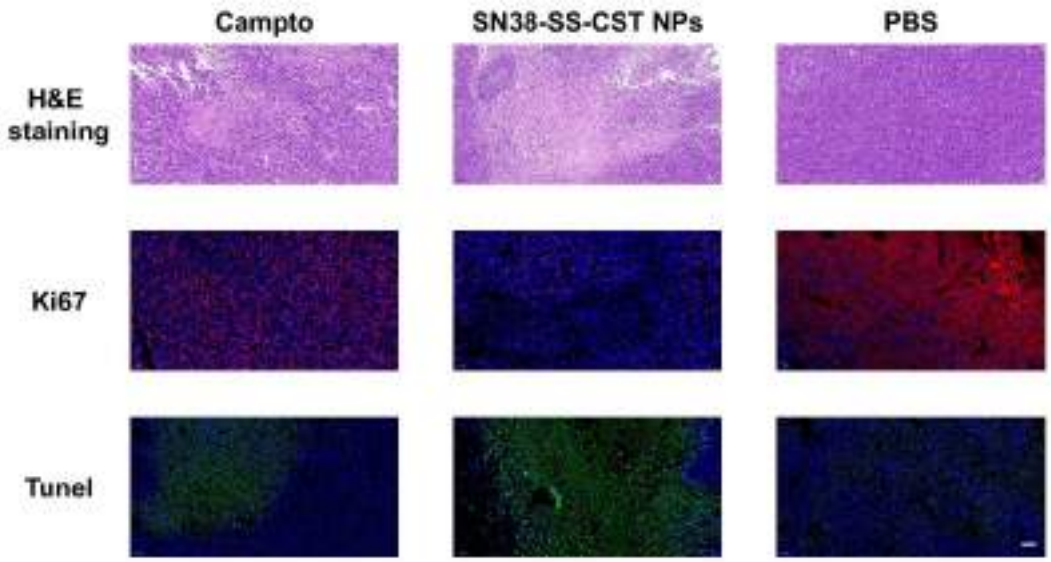

Figure 5. H&E staining, immunofluorescence of ki67 and Tunel of resected CT26 tumors. Scale bar = 50 μm.

3. CONCLUSION

In this work, we developed a tumor redox-responsive carrier-free nanoplatform for the efficient delivery of SN38. First, an endogenous lipid, CST was conjugated with SN38 via a disulfide bond to form SN38-SS-CST prodrug. Through the simple one-step nanoprecipitation

DOI: 10.55415/deep-2023-0010.v1

method, SN38-SS-CST self-assembled in uniform nanoassemblies around 100 nm with good colloidal stability. Under redox environments, SN38-SS-CST NPs could rapidly release active SN38, while showing no burst release under normal physiological conditions. Finally, SN38-SS-CST NPs demonstrated potent antitumor efficacy on both cell studies and in vivo studies without additional toxic effects. Overall, SN38-SS-CST NPs overcame the dilemma of commercial Campto and highlighted the translational prospective.

4. MATERIALS AND METHODS

4.1 Materials

SN38, 3-(4,5-dimethylthiazol-2-yl)-2,5-diphenyl tetrazolium bromide (MTT) was purchased from Dalian Meilun Biotechnology Co., Ltd. CST, 4,4'-dithiodibutyric acid, 4-dimethylaminopyridine were purchased from Macklin Co., Ltd. 1-ethyl-3(3-dimethylpropylamine) carbodiimide and 1-hydroxybenzotriazole were purchased from Aladdin Co., Ltd. 1,2-distearoylsn–glycero-3-phosphoethanolamine-N-methyl (polyethylene glycol)-2000 (DSPE-PEG_{2k}) were obtained from Shanghai Advanced Vehicle Technology Pharmaceutical Ltd. (Shanghai, China). Other reagents in this study were of analytical grade.

4.2 Chemical synthesis

The chemical synthesis of SN38-SS-CST prodrug referred to Figure S1. First, 4,4'-dithiodibutyric acid (0.5 mmol) and acetic anhydride (5 mL) were mixed and stirred in room temperature for 4 h. Then, acetic anhydride was removed by rotary evaporation to obtain 4,4'-dithiodibutyric anhydride. Afterwards, 4,4'-dithiodibutyric anhydride, 4-dimethylaminopyridine (0.15 mmol) and CST (0.6 mmol) were dissolved in anhydrous dichloromethane. The reaction was contained in room temperature for 12 h under stirring. The completion of the reaction was monitored by thin layer chromatography. Finally, the product was extracted and separated by column chromatography (dichloromethane-methanol as mobile phase). The product (CST-SS-COOH) was white solid (yield 73%). The chemical structure of CST-SS-COOH was identified using NMR.

Then, SN38 (0.3 mmol), 1-ethyl-3(3-dimethylpropylamine) carbodiimide (0.4 mmol),

DOI: 10.55415/deep-2023-0010.v1

4-dimethylaminopyridine (0.1 mmol), 1-hydroxybenzotriazole (0.3 mmol) and CST-SS-COOH (0.3 mmol) were dissolved in anhydrous dichloromethane. The reaction was contained in in room temperature for 12 h under stirring. After the completion of the reaction, the product was extracted and separated by preparative liquid chromatography (acetonitrile as mobile phase). The product (SN38-SS-CST) was yellow solid (yield 56%). The chemical structure of SN38-SS-CST was identified using MS and NMR. The purity of SN38-SS-CST was assessed by high performance liquid chromatography (HPLC) at the wavelength of 365 nm.

4.3 Preparation and characterization of prodrug nanoassemblies

Prodrug nanoassemblies of SN38-SS-CST were prepared by the typical one step nano-precipitation method. In brief, SN38-SS-CST (2 mg) was dissolved in 300 μL of acetone, and DSPE-PEG_{2k} (0.5 mg, 20% w/w) was dissolved in 100 μL of ethanol. The drug-containing solution was then mixed and added dropwise to 2 ml of aqueous solution under vigorous stirring for 10 mins. The organic solvent was removed by rotary evaporation to obtain SN38-SS-CST NPs. The dye-labeled prodrug nanoassemblies were prepared using the same procedure by additionally adding coumarin-6 (C-6) into the drug-containing solution. The particle size and zeta potential of SN38-SS-CST NPs were assessed using a Zetasizer. The morphology of SN38-SS-CST NPs was observed using transmission electron microscope (TEM). The sample for observation was aforehand stained with 2% phosphotungstic acid.

4.4 Self-assembly mechanisms

The self-assembly mechanisms of SN38-SS-CST NPs were investigated using molecular dynamics simulations. First, the 3-dimentional conformation of SN38-SS-CST was assesses using Sybyl software. Then, the self-assembly process of SN38-SS-CST NPs was analyzed using Discovery Studio 2017 Visualizer software. The simulated box center parameter was (-6.049, 0.406, 0.869). The simulated box size parameter was (48.897, 40.062, 39.957). The maximum output conformation number is 9.

4.5 Colloidal stability of prodrug nanoassemblies

DOI: 10.55415/deep-2023-0010.v1

To investigate the storage stability of SN38-SS-CST NPs, the samples were sustained at 4℃ for 15 days. The particle size of prodrug nanoassemblies was measured on the 0, 3, 5, 7, 15 day. To investigate the colloidal stability of SN38-SS-CST NPs in biological condition, PBS (pH 7.4) containing 10% Fetal bovine serum (FBS) was used as media. SN38-SS-CST NPs were placed in the PBS containing 10% FBS media at 37℃ under shaking. The samples were collected and the particle size and zeta potential were measured at the 0, 1, 2, 4, 8, 12 h.

4.6 In vitro drug release

To investigated the stimuli-responsiveness of SN38-SS-CST NPs, PBS-ethanol solution (80: 20, v/v) containing no or H2O2 or DTT as stimuli (1, 5, 10 mM) was used as media. Briefly, SN38-SS-CST NPs (200 μg/mL, SN38 equivalent) was placed in the release media at 37℃ under shaking. At selected time intervals (1, 2, 4, 8, 12, 24 h), samples were collected (n = 3 for each group). The concentration of released SN38 was determined by HPLC at the wavelength of 365 nm.

4.7 Cell culture

CT26 colon tumor cells were purchased from Dalian Meilun Biotechnology Co., Ltd (Dalian, China). 4T1 breast tumor cells were purchased from COBIOER Biotechnology Co., Ltd. (Nanjing, China). The cells were cultured in Gibco RPMI 1640 medium containing 10% FBS, streptomycin (100 μg/mL) and penicillin (100 units/mL). The cells were sustained in a cell incubator of 37 °C under 5% CO2 atmosphere.

4.8 Cytotoxicity

The cytotoxicity of SN38-SS-CST NPs and Campto was investigated on CT26 and 4T1 cells by MTT assay. The cells were pre-seeded into 96-well plates (3000 cells per well) and incubated for 24 h before treatment. Then, the media was discarded and replaced with drug-containing media in different concentrations. After the incubation for another 48 h, the drug-containing media was discarded and 25 μL MTT solution (5 mg/mL) was added to each well for another incubation of 4 h. Finally, MTT solution was discarded and 200 μL of DMSO was added to each well. After shaking, the absorbance at 570 nm was detected by a

DOI: 10.55415/deep-2023-0010.v1

microplate reader. The IC50 values were calculated using GraphPad prism 8.0 software.

4.9 Cellular uptake

The cellular uptake efficiency of prodrug nanoassemblies was investigated on CT26 cells using C-6-labeled SN38-SS-CST NPs and C-6 solution. First, CT26 cells were seeded in 24-well plates (5 × 104 cells per well) and incubated for 24 h before treatment. Then, the media was discarded and replaced with C-6-labeled SN38-SS-CST NPs or C-6 solution (250 ng/ml, C-6 equivalent). After an incubation of 0.5 h and 4 h, cells were washed with cold PBS for three times and 4% formaldehyde was used to fix the cells. After another wash process, Hoechst was used to counterstain the nuclei. The prepared slips were observed using CLSM.

4.10 Animal studies

The animal studies in this study were carried out under the guidance and supervision of the Institutional Animal Ethical Care Committee (IAEC) of Shenyang Pharmaceutical University.

4.11 In vivo antitumor efficacy

The antitumor efficacy of SN38-SS-CST NPs and Campto was investigated on xenografted CT26 tumor models. To constructed the CT26 tumor models, CT26 cells (5 × 106 cells per 100 μL) were seeded subcutaneously onto the flank of male BALB/c mice. When the tumor volume was reached around 100 mm3, the treatment started. SN38-SS-CST NPs and Campto were given to the mice every other day (3 mg/kg, SN38 equivalent) for total five injections (n = 8 for each group). Tumor volume and body weight were monitored during the treatment. At two days post last treatment, the mice were scarified. Blood samples were collected and major organs including heart, liver, spleen, lung and kidney as well as tumors were collected. The tumors were weighted. Hepatorenal functions, H&E staining and immunofluorescence staining were conducted by Servicebio Co., Ltd (Wuhan, China). Tumor volume = Long dimeter × Short dimeter2 / 2. Tumor Burden = Tumor weight / Mouse weight.

4.12 Statistical Analysis

All data were presented as mean ± SD. Statistical analysis was assed using GraphPad prism

DOI: 10.55415/deep-2023-0010.v1

8.0 software by one-way analysis of variance (ANOVA) and Student's t-test (two-tailed). Statistical differences were admitted when $p < 0.05$ (*$p < 0.05$, **$p < 0.005$, ***$p < 0.001$, ****$p < 0.0001$).

Acknowledgements

This work was supported by National Natural Science Foundation of China (no. 82272151, 82204318, 82173766), Doctoral Scientific Research Staring Foundation of Liaoning Province (no. 2021-BS-130), General Program of Department of Education of Liaoning Province (no. LJKZ0953), Shenyang Young and Middle-aged Science and Technology Innovation Talent Support Program (no. RC220389).

Conflict of Interest

The authors declare no conflict of interest.

References

[1] Bocci G, Kerbel RS. Pharmacokinetics of metronomic chemotherapy: a neglected but crucial aspect. Nature Reviews Clinical Oncology. 2016.

[2] Voigt W, Matsui S, Yin MB, Burhans WC, Rustum YM. Topoisomerase-I inhibitor SN-38 can induce DNA damage and chromosomal aberrations independent from DNA synthesis. Anticancer Research. 1998;18:3499.

[3] Laizure SC, Herring V, Hu Z, Witbrodt K, Parker RB. The role of human carboxylesterases in drug metabolism: have we overlooked their importance? Pharmacotherapy. 2013;33.

[4] Crawford J, Dale DC, Lyman GH. Chemotherapy-induced neutropenia: risks, consequences, and new directions for its management. Cancer. 2004;100:228.

[5] Sugiyama Y, Kato Y, Chu XY. Multiplicity of biliary excretion mechanisms for the camptothecin derivative irinotecan (CPT-11), its metabolite SN-38, and its glucuronide: role of canalicular multispecific organic anion transporter and P-glycoprotein. Cancer Chemotherapy & Pharmacology. 1998;42:S44-S9.

DOI: 10.55415/deep-2023-0010.v1

[6] Yang W, Yang Z, Liu J, Liu D, Wang Y. Development of a method to quantify total and free irinotecan and 7-ethyl-10-hydroxycamptothecin(SN-38)for pharmacokinetic and bio-distribution studies after administration of irinotecan liposomal formulation. Asian Journal of Pharmaceutical Sciences. 2019;14:687-97.

[7] Slatter JG, Su P, Sams JP, Schaaf LJ, Wienkers LC. Bioactivation of the Anticancer Agent CPT-11 to SN-38 by Human Hepatic Microsomal Carboxylesterases and the in Vitro Assessment of Potential Drug Interactions. Drug Metabolism and Disposition. 1997;25:1157-64.

[8] Jong W. Drug delivery and nanoparticles: Applications and hazards. International Journal of Nanomedicine. 2008;3.

[9] Couvreur P. Nanoparticles in drug delivery: Past, present and future. Advanced drug delivery reviews. 2012;65:21-3.

[10] Zheng Y, Cao T, Han X, Cao P, Zhan Q. Structurally diverse polydopamine-based nanomedicines for cancer therapy. Acta Materia Medica. 2022.

[11] Zhou S, Shang Q, Wang N, Li Q, Song A, Luan Y. Rational design of a minimalist nanoplatform to maximize immunotherapeutic efficacy: Four birds with one stone. Journal of Controlled Release. 2020;328:617-30.

[12] Sun Q, Zhou Z, Qiu N, Shen Y. Rational Design of Cancer Nanomedicine: Nanoproperty Integration and Synchronization. Advanced Materials. 2017;29:1606628.

[13] Fu M, Han X, Chen B, Guo L, Zhong L, Hu P, et al. Cancer treatment: from traditional Chinese herbal medicine to the liposome delivery system. Acta Materia Medica. 2022.

[14] Fu S, Li G, Zang W, Zhou X, Shi K, Zhai Y. Pure drug nano-assemblies: A facile carrier-free nanoplatform for efficient cancer therapy. Acta Pharmaceutica Sinica B. 2021.

[15] Li Y, Li L, Jin Q, Liu T, Sun J, Wang Y, et al. Impact of the amount of PEG on prodrug nanoassemblies for efficient cancer therapy. Asian Journal of Pharmaceutical Sciences. 2022;17:241-52.

[16] Li Y, Kang T, Wu Y, Chen Y, Zhu J, Gou M. Carbonate Ester Turn Camptothecin-unsaturated Fatty Acid Prodrug into Nanomedicine for Cancer Therapy. Chemical Communications. 2018:10.1039.C8CC00639C.

DOI: 10.55415/deep-2023-0010.v1

[17] Sarwar H, Khalid HM, Basher MK, Mia M, Rahman MT, Jalal UM. Smart nanocarrier-based drug delivery systems for cancer therapy and toxicity studies: A review. Journal of Advanced Research. 2018;15:1-18.

[18] Li G, Sun B, Li Y, Luo C, He Z, Sun J. Small-Molecule Prodrug Nanoassemblies: An Emerging Nanoplatform for Anticancer Drug Delivery. Small.

[19] Yang Y, Zuo S, Zhang J, Liu T, Li X, Zhang H, et al. Prodrug nanoassemblies bridged by Mono-/Di-/Tri-sulfide bonds: Exploration is for going further. Nano Today. 2022;44:101480.

[20] He Q, Chen J, Yan J, Cai S, Mo M. Tumor microenvironment responsive drug delivery systems. Asian Journal of Pharmaceutical Sciences. 2019;15.

[21] Zhang M, Qin X, Zhao Z, Du Q, Li Q, Jiang Y, et al. A self-amplifying nanodrug to manipulate the Janus-faced nature of ferroptosis for tumor therapy. Nanoscale horizons. 2022;7:198-210.

[22] Sun B, Luo C, Zhang X, Guo M, Sun M, Yu H, et al. Probing the impact of sulfur/selenium/carbon linkages on prodrug nanoassemblies for cancer therapy. Nature communications. 2019;10:1-10.

[23] Kumar R, Han J, Lim HJ, Ren WX, Lim JY, Kim JH, et al. Mitochondrial induced and self-monitored intrinsic apoptosis by antitumor theranostic prodrug: in vivo imaging and precise cancer treatment. Journal of the American Chemical Society. 2014;136:17836.

[24] Boyle ST, Johan MZ, Samuel MS. Tumour-directed microenvironment remodelling at a glance. Journal of Cell Science. 2020;133:jcs247783.

[25] Du J, Lane LA, Nie S. Stimuli-responsive nanoparticles for targeting the tumor microenvironment. Journal of Controlled Release. 2015;219:205-14.

[26] Li C, Wang J, Wang Y, Gao H, Wei G, Huang Y, et al. Recent progress in drug delivery. Acta pharmaceutica sinica B. 2019;9:1145-62.

[27] Sun, Bingjun, Luo, Cong, Yu, Han, et al. Disulfide Bond-Driven Oxidation- and Reduction-Responsive Prodrug Nanoassemblies for Cancer Therapy. Nano Letters. 2018.

[28] Li G, Sun B, Zheng S, Xu L, Tao W, Zhao D, et al. Zwitterion‐driven shape program of prodrug nanoassemblies with high stability, high tumor accumulation, and high antitumor activity. Advanced Healthcare Materials. 2021;10:2101407.

DOI: 10.55415/deep-2023-0010.v1